

Kinematic and Dynamic Study of an Inertial System Transforming Rotational Motion into Unidirectional Linear Motion

Attila GERŐCS, Elena MUNCUT (WISZNOVSZKY)*, Andrei KOMJATY, Ramona LILE, István BÍRÓ

Abstract In this paper we would like to present some lesser-known aspects of inertial systems for transforming rotational motion into unidirectional (linear) translational motion by using a device (inertial system) using weights mounted on the chain of a chain drive, which is made in 3D format. Cylindrical and bevel gear drives are also used in the system. The study of the problem was done by mathematical modeling in MathCAD of the displacement, velocity, acceleration and inertia force and by making the graphical scheme of the system in AutoCAD and SolidWorks.

Keywords: inertial system; mathematical modeling; rotational motion; translational motion

1 INTRODUCTION

This system is an innovation made by the authors. The inertial systems for transforming rotational motion into unidirectional linear motion are an area of engineering that has been of increasing interest to engineers and researchers in recent decades. These systems are multi-body systems with accelerated masses, i.e. masses slowed down in a well-defined direction which is also the direction of motion of the system. The accelerated and slowed-down masses produce inertial forces in the system, respectively reaction forces that ensure the linear displacement of the system.

This system defies the laws of Newtonian mechanics and because of this there is controversy over the operation of these inertial systems. More than a hundred such patented inertial systems are known but only very few have been realized in practice.

These systems use solid [1, 2] or liquid [1, 3, 4] respectively accelerated and decelerated masses for the unidirectional translational motion and the energy used for them may be mechanical energy [2, 5, 6] or mechanical energy combined with electromagnetic energy [7].

In this paper we will make a kinematic and dynamic study of an inertial system, [8] that provides the displacement of a device on which this system is mounted, [9, 10], wherever possible inside the vehicle, we need to build a kinematic chain between this system and the vehicle wheels, only a kinematic connection between the drive engine and the system.

1.1 Description of the System

To describe the system, we will use: the principle diagram in two views (Fig. 1) and the presentation of the positions of the weights on the chain (Fig. 2) in different angular positions of rotation of the chain plane around an axis of symmetry of the chain (Fig. 3a, b, c and d).

The system, as shown in Fig. 1 and Fig. 2, consists of a chassis 14 on which a bevel gear 1 is fixedly mounted. The central reaming of this gear 1 carries the axis of rotation of a mobile frame 6 in the form of a crank handle. On this frame is mounted the common axis (shaft) of rotation of the wheels 2 (bevel gear) and 4 (chain wheel) respectively. The bevel gear is thus mounted so as to act as a satellite wheel forming a gearing with bevel gear 1.

The chain wheel 4 transmits the rotational movement by means of chain 5 to chain wheel 3. The axis of rotation of the chain wheel is mounted at one end of the frame 6, which rotates the chain wheel 7 also mounted on this axis.

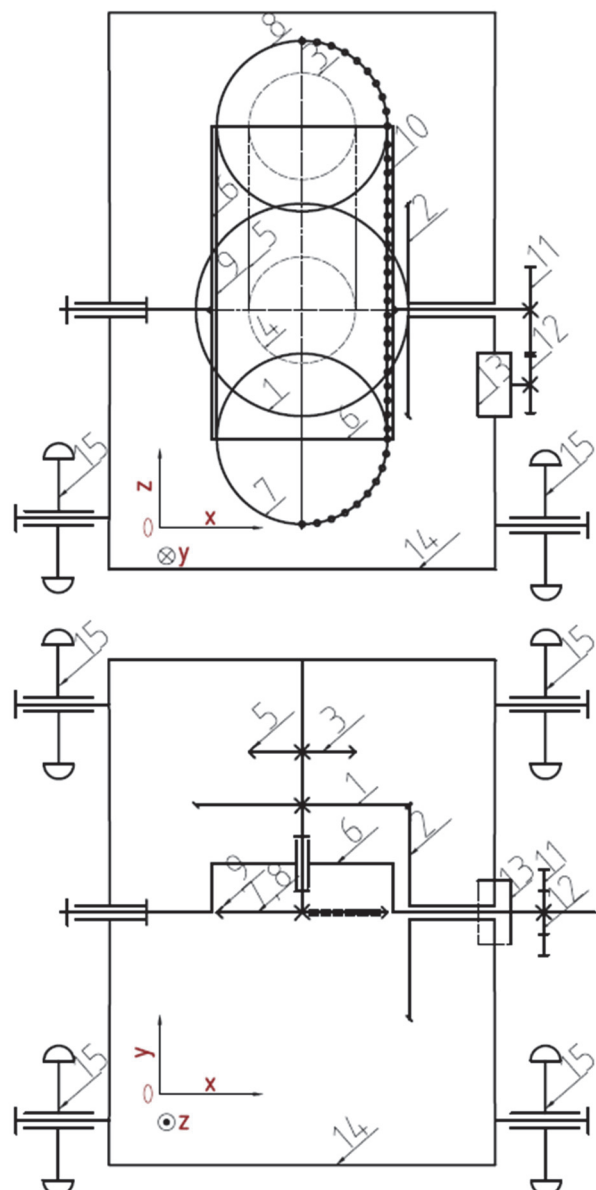


Figure 1 Scheme of the mechanical system

On the other end of the frame 6 the chain wheel 8 is mounted, fixed on a mobile axis. The connection between the two chain wheels 7 and 8 respectively is made by means of the chain 9 to which weights 10 are mounted on the half-length.

The transmission ratios, i.e. the dimensions of the component parts of the system, are such that when the frame 6 is rotated completely, the chain wheel 9 executes half a displacement, i.e. the weighted portion replaces the unweighted portion and vice versa. The frame 6 is set in

rotational motion by means of a motor 13 via a gearing with cylindrical gears 11 and 12.

Four running wheels 15 are mounted on the chassis 14 to ensure the linear movement of the system.

The elements used in mathematical modelling are as follows: $R = 0,3 \text{ m}$ - chain wheel splitting radius 7, respectively 8, $\omega = 100 \text{ rad/s}$ - angular velocity 6, $M = 5 \text{ kg}$ - the total mass of the weights uploaded on the chain 9.

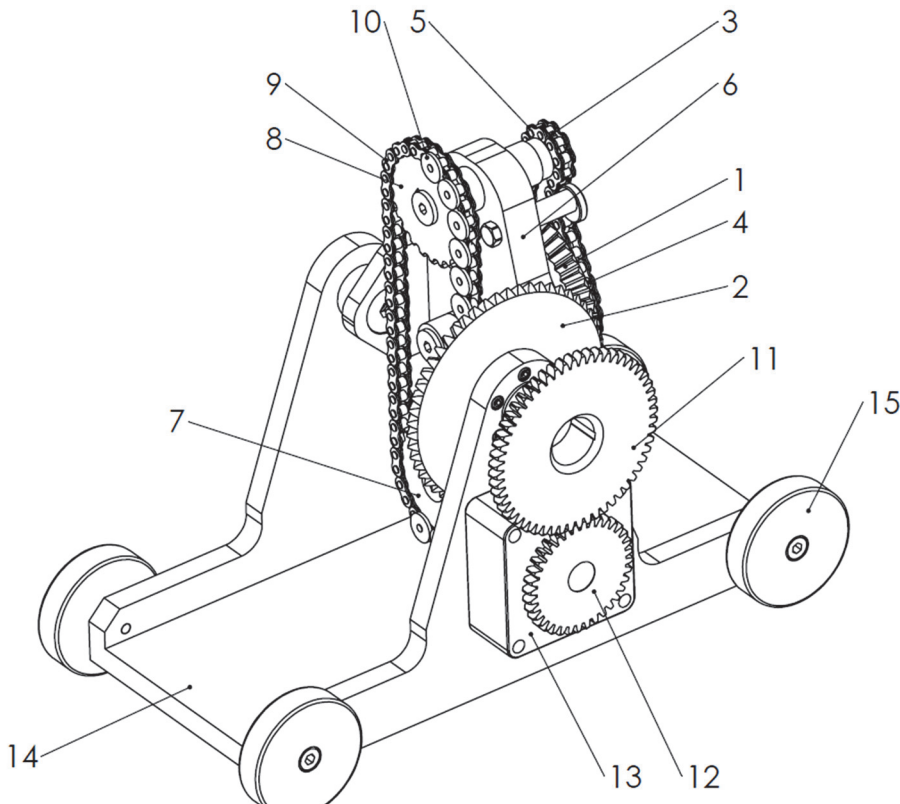


Figure 2 3D representation of the mechanical system

According to Fig. 3a₂ it is sufficient to consider the equation of displacement along the axis Oy of the center of gravity of the portion $a \div b$ of the chain equipped with weights, in an intermediate position in the range $\omega t_1 \in \left(0; \frac{\pi}{4}\right)$, also $2\omega t_1 \in \left(0; \frac{\pi}{2}\right)$ because the portion $c \div d$ of the weighted chain is symmetrical with respect to the axis of rotation of frame 6 (because as the circle arc equipped with weights increases $a \div a'$ the more the weightless arc portion increases $c' \div c$).

According to Fig. 3b₂ which is an intermediate position of the chain with weights in the range $\omega t_2 \in \left(\frac{\pi}{4}; \frac{\pi}{2}\right]$ namely $2\omega t_2 \in \left[\frac{\pi}{2}; \pi\right]$ we have to write the equation of displacement along the direction of the Oy axis of the center of gravity of the part of the chain equipped with weights $a \div b$ and $b \div c$ with the mention that the multiplication of the acceleration of the center of gravity of the portion $a \div b$, with the mass of this portion we must consider the product double, because the portion of the chain with weights $c \div d$ also appears, which behaves the

same as the portion $a \div b$ being the same length and is positioned identically to the axis of rotation of the frame 6 as a portion $a \div b$ and the portion $d \div e$ is symmetrical to the axis of rotation of the frame 6, so this portion no longer needs to be taken into account.

According to Fig. 3c₂ which is an intermediate position of the chain in the range $\omega t_3 \in \left[\frac{\pi}{2}; \frac{3\pi}{4}\right]$, also

$2\omega t_3 \in \left[\pi; \frac{3\pi}{2}\right]$ we have to write the equations of motion

along the direction of the Oy axis of the centers of gravity of the weighted chain portion $b \div c$ and $c \div d$ with the mention that when multiplying the acceleration of the center of gravity of the portion $b \div c$ with the mass of this portion the product must be doubled because there appears the portion $d \div e$ identical in position and mass to the portion $b \div c$.

According to Fig. 3d₂ which is an intermediate position of the chain $\omega t_4 \in \left[\frac{3\pi}{4}; \pi\right]$, also $2\omega t_4 \in \left[\frac{3\pi}{2}; 2\pi\right]$

it is sufficient to write the equation of motion of the center

of gravity of the portion $d \div f$ because the portion a to d is symmetrical to the axis of rotation of frame 6, so it does not need to be taken into account.

Starting with $\omega t = \pi$ until $\omega t = 2\pi$ the phenomenon is repeated from a) to d).

In order to obtain the tractive force along the direction Oy, it is necessary that the arithmetic mean value of the sums of all the weights on the chain considered at a rotation of 180° of the chain plane gives a negative value. It is sufficient to study the system at one rotation of the chain plane, only 180° because at further rotation up to 360° the phenomena performed by the system are repeated, the tractive force obtained having the same direction and value.

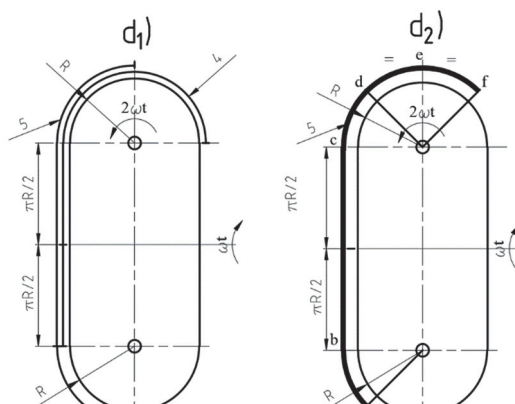
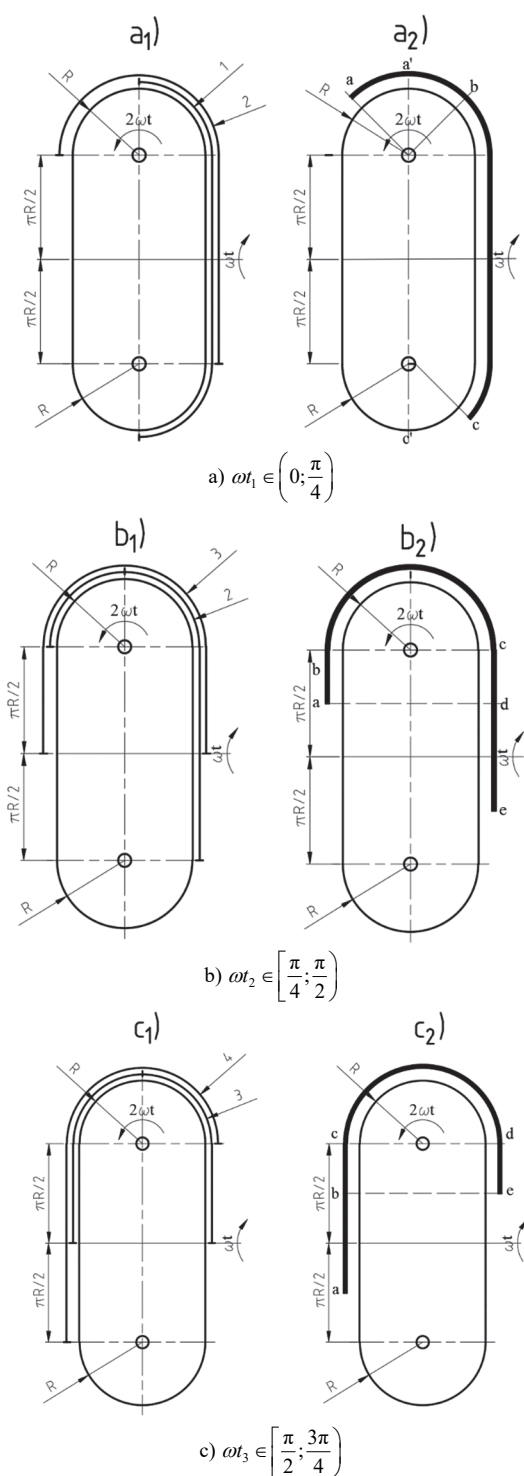


Figure 3 Way of moving the chain parts with weights -Rotation interval

In order to not determine the displacements, velocities and accelerations of each weight on the chain, it is sufficient and simpler to study the movements of the centers of gravity of the various simple portions occupied by the weights on the chain. Centers of gravity of these portions, mentioned above, being considered straight bars and arcs of circles occupied by weights of the chain, can be easily established.

Of course, in this case the masses of these weighted portions also change during the chain's rotation.

The ends of the portions of the chain with weights where the formulas for determining the accelerations of the centers of weights changes the shape are shown in Fig. 3a, b, c and d.

2 MATHEMATICAL MODELLING OF INERTIA FORCE

The displacement equations according to the direction of the Oy axis of the gravity centers of the various portions of the chain which can be identified by simple volumes, can be written:

$$\text{Range 1.} \rightarrow \alpha_1 = \omega t_1 \in \left(0; \frac{\pi}{4}\right]; 2\omega t_1 \in \left(0; \frac{\pi}{2}\right] \quad (1)$$

$$y_1(t_1) = \left(R \cdot \frac{\sin 2\omega t_1 + \pi R}{2\omega t_1} \right) \cdot \sin \omega t_1 \quad (2)$$

$$\text{Range 2.} \rightarrow \alpha_2 = \omega t_2 \in \left(\frac{\pi}{4}; \frac{\pi}{2}\right]; 2\omega t_2 \in \left(\frac{\pi}{2}; \pi\right] \quad (3)$$

$$y_2(t_2) = \left(\frac{\pi R}{2} - \frac{\left(2\omega t_2 - \frac{\pi}{2}\right) \cdot R}{2} \right) \cdot \sin \omega t_2 + \\ + \left(R \cdot \frac{\sin \frac{\pi}{2} + \frac{\pi \cdot R}{2}}{\frac{\pi}{2}} \right) \cdot \sin \omega t_2 \quad (4)$$

where:

$$y_{2A}(t_2) = \left(\frac{\pi \cdot R}{2} - \frac{(2\omega t_2 - \frac{\pi}{2}) \cdot R}{2} \right) \cdot \sin \omega t_2 \quad (5)$$

$$y_{2B}(t_2) = \left(R \cdot \frac{\sin \frac{\pi}{2}}{\frac{\pi}{2}} + \frac{\pi \cdot R}{2} \right) \cdot \sin \omega t_2 \quad (6)$$

$$\text{Range 3.} \rightarrow \alpha_3 = \omega t_3 \in \left[\frac{\pi}{2}; \frac{3\pi}{4} \right]; 2\omega t_3 \in \left[\frac{\pi}{1}; \frac{3\pi}{2} \right] \quad (7)$$

$$y_3(t_3) = \left(\frac{\pi \cdot R}{4} + \frac{(2\omega t_3 - \pi) \cdot R}{2} \right) \cdot \sin \omega t_3 + \\ + \left(R \cdot \frac{\sin \frac{\pi}{2}}{\frac{\pi}{2}} + \frac{\pi \cdot R}{2} \right) \cdot \sin \omega t_3 \quad (8)$$

$$y_{3A}(t_3) = \left(\frac{\pi \cdot R}{4} + \frac{(2\omega t_3 - \pi) \cdot R}{2} \right) \cdot \sin \omega t_3 \quad (9)$$

$$y_{3B}(t_3) = \left(R \cdot \frac{\sin \frac{\pi}{2}}{\frac{\pi}{2}} + \frac{\pi \cdot R}{2} \right) \cdot \sin \omega t_3 \quad (10)$$

$$\text{Range 4.} \rightarrow \alpha_4 = \omega t_4 \in \left[\frac{3\pi}{4}; \pi \right]; 2\omega t_4 \in \left[\frac{3\pi}{2}; 2\pi \right] \quad (11)$$

$$y_4(t_4) = \left(R \cdot \frac{\sin \left(\frac{\pi}{2} - \left(2\omega t_4 - \frac{3\pi}{2} \right) \right)}{\left(\frac{\pi}{2} - \left(2\omega t_4 - \frac{3\pi}{2} \right) \right)} + \frac{\pi R}{2} \right) \cdot \sin \omega t_4 \quad (12)$$

Since the mass of these weighted portions of the chain also varies with time, the formulas of the masses (Eq. (13) - (20)), if we consider the mass per unit length of the chain.

$$m_1(t_1) = 2\omega t_1 \cdot \frac{M}{\pi} \quad (13)$$

$$m_2(t_2) = (2\omega t_2 - \frac{\pi}{2}) \cdot \frac{M}{\pi} + \frac{M}{2} \quad (14)$$

$$m_{2A}(t_2) = (2\omega t_2 - \frac{\pi}{2}) \cdot \frac{M}{\pi} \quad (15)$$

$$m_{2B}(t_2) = \frac{M}{2} \quad (16)$$

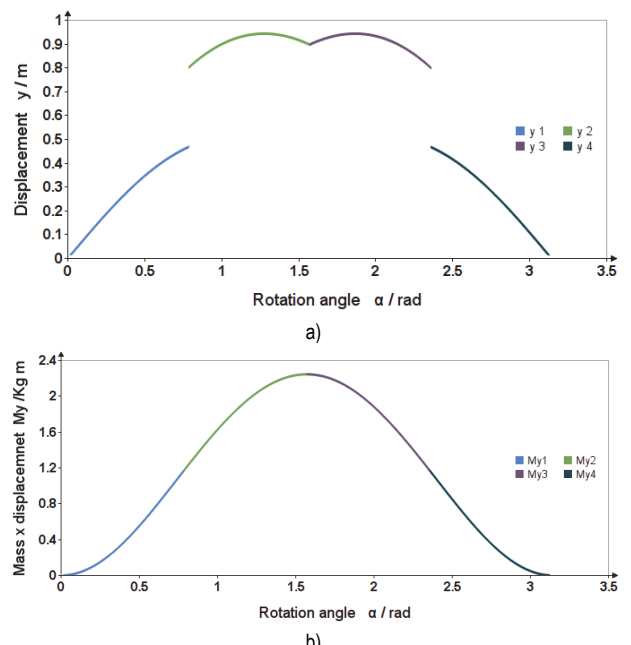


Figure 4 a) Representation of displacement over the whole range, b) Representation of mass multiplied by displacement

$$m_3(t_3) = m_{3A}(t_3) + m_{3B}(t_3) = \\ = \left(\frac{\pi R}{2} - (2\omega t_3 - \pi) \cdot R \right) \cdot \frac{M}{\pi R} + \frac{M}{2} \quad (17)$$

$$m_{3A}(t_3) = \left(\frac{\pi R}{2} - (2\omega t_3 - \pi) \cdot R \right) \cdot \frac{M}{\pi R} \quad (18)$$

$$m_{3B}(t_3) = \frac{M}{2} \quad (19)$$

$$m_4(t_4) = \frac{M}{2} - 2 \cdot \left(2\omega t_4 - \frac{3\pi}{2} \right) \cdot \frac{M}{\pi} \quad (20)$$

$$v_{y1}(t_1) = \dot{y}_1 = -\frac{R \cdot \sin \omega t_1 \cdot \sin 2\omega t_1}{2\omega t_1^2} + \\ + \frac{R \cdot \cos \omega t_1 \cdot \sin 2\omega t_1}{2t_1} + \frac{R \cdot \cos 2\omega t_1 \cdot \sin \omega t_1}{t_1} + \\ + \frac{\omega \cdot R \cdot \pi \cdot \cos \omega t_1}{2} \quad (21)$$

$$v_{y2}(t_2) = v_{y2A} + v_{y2B} = y_2 = \\ = \frac{-(4 \cdot \omega \cdot R \cdot \sin \omega t_2)}{4} + \\ + \frac{(3 \cdot \omega \cdot R \cdot \pi - 4 \cdot \omega^2 \cdot R \cdot t_2) \cdot \cos \omega t_2}{4} + \\ + \frac{(\omega \cdot R \cdot \pi^2 + 4 \cdot \omega \cdot R) \cdot \cos \omega t_2}{2\pi} \quad (22)$$

where:

$$\begin{aligned} v_{y2A}(t_2) = \dot{y}_{2A} &= \frac{-(4 \cdot \omega \cdot R \cdot \sin \omega t_2)}{4} + \\ &+ \frac{(3 \cdot \omega \cdot R \cdot \pi - 4 \cdot \omega^2 \cdot R \cdot t_2) \cdot \cos \omega t_2}{4} \end{aligned} \quad (23)$$

$$v_{y2B}(t_2) = \dot{y}_{2B} = \frac{(\omega \cdot R \cdot \pi^2 + 4 \cdot \omega \cdot R) \cdot \cos \omega t_2}{2 \cdot \pi} \quad (24)$$

$$\begin{aligned} v_{y3}(t_3) = v_{y3A}(t_3) + v_{y3B}(t_3) &= \frac{4 \cdot \omega \cdot R \cdot \sin \omega t_3}{4} + \\ &+ \frac{(4 \cdot \omega^2 \cdot R \cdot t_3 - \omega \cdot R \cdot \pi) \cdot \cos \omega t_3}{4} \\ &+ \frac{(\omega \cdot R \cdot \pi^2 + 4 \cdot \omega \cdot R) \cdot \cos \omega t_3}{2 \cdot \pi} \end{aligned} \quad (25)$$

where

$$\begin{aligned} v_{y3A}(t_3) &= \frac{4 \cdot \omega \cdot R \cdot \sin \omega t_3}{4} + \\ &+ \frac{(4 \cdot \omega^2 \cdot R \cdot t_3 - \omega \cdot R \cdot \pi) \cdot \cos \omega t_3}{4} \end{aligned} \quad (26)$$

$$v_{y3B}(t_3) = \frac{(\omega \cdot R \cdot \pi^2 + 4 \cdot \omega \cdot R) \cdot \cos \omega t_3}{2\pi} \quad (27)$$

$$\begin{aligned} v_{y4}(t_4) = \dot{y}_4 &= -\frac{(\omega \cdot R \cdot \sin \omega t_4) \cdot \sin 2\omega t_4}{2\pi^2 - 4\omega t_4 \pi + 2\omega^2 t_4^2} - \\ &- \frac{(\omega \cdot R \cdot \pi - \omega^2 \cdot R \cdot t_4) \cdot \cos \omega t_4 \cdot \sin 2\omega t_4}{2\pi^2 - 4\omega t_4 \pi + 2\omega^2 t_4^2} + \\ &+ \frac{(2 \cdot \omega \cdot R \cdot \pi - 2 \cdot \omega^2 \cdot R \cdot t_4) \cdot \cos 2\omega t_4 \cdot \sin \omega t_4}{2\pi^2 - 4\omega t_4 \cdot \pi + 2\omega^2 t_4^2} + \\ &+ \frac{\omega \cdot R \cdot \pi \cdot \cos \omega t_4}{2} \end{aligned} \quad (28)$$

The velocity graph for the 4 positions is obtained as shown in Fig. 5.

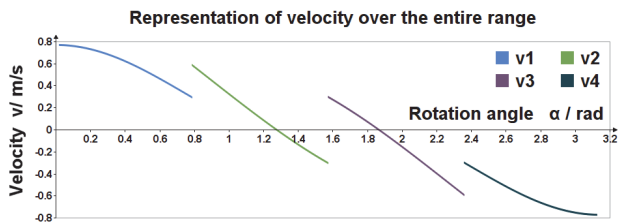


Figure 5 Representation of velocity over the whole range

The determination of the force of inertia will be done according to the impulse theorem, which says that the derivative of the impulse with respect to time is equal to the force at each moment during the motion. The impulse is $\vec{H} = m \cdot \vec{v}$ and the force will be $\dot{\vec{H}} = \vec{F}$.

To be able to calculate the force \vec{F} developed by the device, which is obtained by the 1st-order derivative of the impulse, next we will calculate the impulse for each portion $H_i = m_i \cdot \vec{v}_i$, where $i = 1, 2, 3, 4$.

$$\begin{aligned} H_1(t_1) = m_1(t_1) \cdot v_{y1}(t_1) &= (2 \cdot \omega \cdot t_1) \cdot \frac{M}{\pi} \cdot \\ &\cdot \left[-\frac{R \cdot \sin \omega t_1 \cdot \sin 2\omega t_1}{2\omega t_1^2} + \frac{R \cdot \cos \omega t_1 \cdot \sin 2\omega t_1}{2t_1} + \right. \\ &\left. + \frac{R \cdot \cos 2\omega t_1 \cdot \sin \omega t_1}{t_1} + \frac{\omega \cdot R \cdot \pi \cdot \cos \omega t_1}{2} \right] \end{aligned} \quad (29)$$

$$\begin{aligned} H_2(t_2) = m_2(t_2) \cdot v_{y2}(t_2) &= (2 \cdot \omega \cdot t_2 - \frac{\pi}{2}) \cdot \frac{M}{\pi} \cdot \\ &\cdot \left[\frac{-(4 \cdot \omega \cdot R \cdot \sin \omega t_2)}{4} + \right. \\ &\left. + \frac{(3 \cdot \omega \cdot R \cdot \pi - 4 \cdot \omega^2 \cdot R \cdot t_2) \cdot \cos \omega t_2}{4} \right] + \\ &+ \frac{M}{2} \cdot \frac{(\omega \cdot R \cdot \pi^2 + 4 \cdot \omega \cdot R) \cdot \cos \omega t_2}{2\pi} \end{aligned} \quad (30)$$

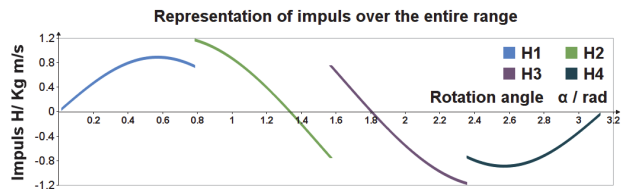


Figure 6 Representation of impuls over the entire range

$$\begin{aligned} H_3(t_3) = m_3(t_3) \cdot v_{y3}(t_3) &= \left(\frac{\pi \cdot R}{2} - (2 \cdot \omega \cdot t_3 - \pi) \cdot R \right) \cdot \frac{M}{\pi R} \cdot \\ &\cdot \left[\frac{4 \cdot \omega \cdot R \cdot \sin \omega t_3}{4} + \right. \\ &\left. + \frac{(4 \cdot \omega^2 \cdot R \cdot t_3 - \omega \cdot R \cdot \pi) \cdot \cos \omega t_3}{4} \right] + \\ &+ \frac{M}{2} \cdot \left[\frac{(\omega \cdot R \cdot \pi^2 + 4 \cdot \omega \cdot R) \cdot \cos \omega t_3}{2\pi} \right] \end{aligned} \quad (31)$$

$$\begin{aligned} H_4(t_4) = m_4(t_4) \cdot v_{y4}(t_4) &= \left[\frac{M}{2} - 2 \cdot (2 \cdot \omega \cdot t_4 - \frac{3 \cdot \pi}{2}) \cdot \frac{M}{\pi} \right] \\ &\cdot \left[-\frac{(\omega \cdot R \cdot \sin(\omega \cdot t_4)) \cdot \sin(2 \cdot \omega \cdot t_4)}{2 \cdot \pi^2 - 4 \cdot \omega \cdot t_4 \cdot \pi + 2 \cdot \omega^2 \cdot t_4^2} - \right. \\ &\left. - \frac{(\omega \cdot R \cdot \pi - \omega^2 \cdot R \cdot t_4) \cdot \cos(\omega \cdot t_4) \cdot \sin(2 \cdot \omega \cdot t_4)}{2 \cdot \pi^2 - 4 \cdot \omega \cdot t_4 \cdot \pi + 2 \cdot \omega^2 \cdot t_4^2} + \right. \\ &\left. + \frac{(2 \cdot \omega \cdot R \cdot \pi - 2 \cdot \omega^2 \cdot R \cdot t_4) \cdot \cos(2 \cdot \omega \cdot t_4) \cdot \sin(\omega \cdot t_4)}{2 \cdot \pi^2 - 4 \cdot \omega \cdot t_4 \cdot \pi + 2 \cdot \omega^2 \cdot t_4^2} + \right. \\ &\left. + \frac{\omega \cdot R \cdot \pi \cdot \cos(\omega \cdot t_4)}{2} \right] \end{aligned} \quad (32)$$

$$\begin{aligned}
F_1(t_1) = & (-1) \cdot \\
& \left[-\frac{\left(5 \cdot t_1^2 \cdot \omega^2 - 1\right) \cdot M \cdot R \cdot \sin \omega t_1 \cdot \sin 2\omega t_1}{t_1^2 \cdot \pi} - \right. \\
& - \frac{t_1 \cdot \omega \cdot M \cdot R \cdot \cos \omega t_1 \cdot \sin 2\omega t_1}{t_1^2 \cdot \pi} + \\
& + \frac{2 \cdot t_1 \cdot \omega \cdot M \cdot R \cdot \cos 2\omega t_1 \cdot \sin \omega t_1}{t_1^2 \cdot \pi} - \\
& - \frac{4 \cdot t_1^2 \cdot \omega^2 \cdot M \cdot R \cdot \cos \omega t_1 \cdot \cos 2\omega t_1}{t_1^2 \cdot \pi} + \\
& \left. + \left(\omega^2 \cdot M \cdot R \cdot \cos \omega t_1 - t_1 \cdot \omega^3 \cdot M \cdot R \cdot \sin \omega t_1\right)\right] \quad (33)
\end{aligned}$$

$$\begin{aligned}
F_2(t_2) = & (-1) \cdot \\
& \left[\frac{(3 \cdot \omega^2 \cdot M \cdot R \cdot \pi^2 - 16 \cdot t_2 \cdot \omega^3 \cdot M \cdot R \cdot \pi) \cdot \sin \omega t_2}{8 \cdot \pi} + \right. \\
& \frac{(16 \cdot t_2^2 \cdot \omega^4 - 16 \cdot \omega^2) \cdot M \cdot R \cdot \sin \omega t_2}{8 \cdot \pi} + \\
& \frac{(28 \cdot \omega^2 \cdot M \cdot R \cdot \pi - 48 \cdot t_2 \cdot \omega^3 \cdot M \cdot R) \cdot \cos \omega t_2}{8 \cdot \pi} + \\
& \left. + \frac{(-(\omega^2 \cdot M \cdot R \cdot \pi^2) - 4 \cdot \omega^2 \cdot M \cdot R) \cdot \sin \omega t_2}{4 \cdot \pi} \right] \quad (34)
\end{aligned}$$

$$\begin{aligned}
F_3(t_3) = & (-1) \cdot \\
& \left[\frac{(3 \cdot \omega^2 \cdot M \cdot R \cdot \pi^2 - 16 \cdot t_3 \cdot \omega^3 \cdot M \cdot R \cdot \pi) \cdot \sin \omega t_3}{8 \cdot \pi} + \right. \\
& \frac{(16 \cdot t_3^2 \cdot \omega^4 - 16 \cdot \omega^2) \cdot M \cdot R \cdot \sin \omega t_3}{8 \cdot \pi} + \\
& \frac{(28 \cdot \omega^2 \cdot M \cdot R \cdot \pi - 48 \cdot t_3 \cdot \omega^3 \cdot M \cdot R) \cdot \cos \omega t_3}{8 \cdot \pi} + \\
& \left. + \frac{(-(\omega^2 \cdot M \cdot R \cdot \pi^2) - 4 \cdot \omega^2 \cdot M \cdot R) \cdot \sin \omega t_3}{4 \cdot \pi} \right] \quad (35)
\end{aligned}$$

By making the first-order derivative of the impuls we obtain the analytical form of the force corresponding to the centres of gravity of the disc portions (weights) along the Oy axis, as shown in Fig. 7.

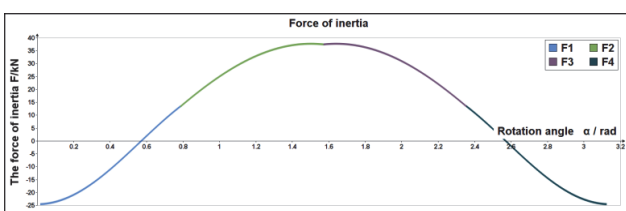


Figure 7 Representation of the force of inertia over the whole range

$$\begin{aligned}
F_4(t_4) = & (-1) \cdot \\
& \left[\frac{\left(5 \cdot \omega^2 \cdot M \cdot R \cdot \pi^2\right) \cdot \sin \omega t_4 \cdot \sin 2\omega t_4}{\pi^3 - 2 \cdot t_4 \cdot \omega \cdot \pi^2 + t_4^2 \cdot \omega^2 \cdot \pi} + \right. \\
& - \frac{10 \cdot t_4 \cdot \omega^3 \cdot M \cdot R \cdot \pi \cdot \sin \omega t_4 \cdot \sin 2\omega t_4}{\pi^3 - 2 \cdot t_4 \cdot \omega \cdot \pi^2 + t_4^2 \cdot \omega^2 \cdot \pi} + \\
& + \frac{\left(5 \cdot t_4^2 \cdot \omega^4 - \omega^2\right) \cdot M \cdot R \cdot \sin \omega t_4 \cdot \sin 2\omega t_4}{\pi^3 - 2 \cdot t_4 \cdot \omega \cdot \pi^2 + t_4^2 \cdot \omega^2 \cdot \pi} + \\
& + \frac{\left(t_4 \cdot \omega^3 \cdot M \cdot R - \omega^2 \cdot M \cdot R \cdot \pi\right) \cdot \cos \omega t_4 \cdot \sin 2\omega t_4}{\pi^3 - 2 \cdot t_4 \cdot \omega \cdot \pi^2 + t_4^2 \cdot \omega^2 \cdot \pi} + \\
& + \frac{\left(2 \cdot t_4 \cdot \omega^3 \cdot M \cdot R - 2 \cdot \omega^2 \cdot M \cdot R \cdot \pi\right) \cdot \cos 2\omega t_4 \cdot \sin \omega t_4}{\pi^3 - 2 \cdot t_4 \cdot \omega \cdot \pi^2 + t_4^2 \cdot \omega^2 \cdot \pi} + \\
& + \frac{\left(8 \cdot t_4 \cdot \omega^3 \cdot M \cdot R \cdot \pi - 4 \cdot \omega^2 \cdot M \cdot R \cdot \pi^2\right) \cdot \cos \omega t_4 \cdot \cos 2\omega t_4}{\pi^3 - 2 \cdot t_4 \cdot \omega \cdot \pi^2 + t_4^2 \cdot \omega^2 \cdot \pi} - \\
& - \frac{4 \cdot t_4^2 \cdot \omega^4 \cdot M \cdot R \cdot \cos \omega t_4 \cdot \cos 2\omega t_4}{\pi^3 - 2 \cdot t_4 \cdot \omega \cdot \pi^2 + t_4^2 \cdot \omega^2 \cdot \pi} + \\
& \left. + \left[\left(t_4 \cdot \omega^3 \cdot M \cdot R - \omega^2 \cdot M \cdot R \cdot \pi\right) \cdot \sin \omega t_4 - \right. \right. \\
& \left. \left. - \omega^2 \cdot M \cdot R \cdot \cos \omega t_4 \right] \right] \quad (36)
\end{aligned}$$

$$\begin{aligned}
& \int_0^{\frac{\pi}{4}} F_1(\alpha_1) d\alpha_1 + \int_{\frac{\pi}{4}}^{\frac{\pi}{2}} F_2(\alpha_2) d\alpha_2 + \\
& + \int_{\frac{\pi}{2}}^{\frac{3\pi}{4}} F_3(\alpha_3) d\alpha_3 + \int_{\frac{3\pi}{4}}^{\pi} F_4(\alpha_4) d\alpha_4 = 23.597 \text{ kN} \quad (37)
\end{aligned}$$

Considering the independent linear system $S = \{u_1, u_2, u_3, u_4\}$ with [11]:

$$u_1(\alpha_1) = \begin{bmatrix} \alpha_1 \\ v_1(\alpha_1) \\ F_1(\alpha_1) \end{bmatrix} \text{ were } \alpha_1 \in \left(0; \frac{\pi}{4}\right) \quad (38)$$

$$u_2(\alpha_2) = \begin{bmatrix} \alpha_2 \\ v_2(\alpha_2) \\ F_2(\alpha_2) \end{bmatrix} \text{ were } \alpha_2 \in \left[\frac{\pi}{4}; \frac{\pi}{2}\right) \quad (39)$$

$$u_3(\alpha_3) = \begin{bmatrix} \alpha_3 \\ v_3(\alpha_3) \\ F_3(\alpha_3) \end{bmatrix} \text{ were } \alpha_3 \in \left[\frac{\pi}{2}; \frac{3\pi}{4}\right) \quad (40)$$

$$u_4(\alpha_4) = \begin{bmatrix} \alpha_4 \\ v_4(\alpha_4) \\ F_4(\alpha_4) \end{bmatrix} \text{ were } \alpha_4 \in \left[\frac{3\pi}{4}; \pi\right) \quad (41)$$

Dependence of force on angle of rotation and linear speed of movement of the module used the $\text{curve}(\alpha)$ and

CreateSpace function in Mathcad where we also imposed the angels' intervals for each inertial force, Fig. 8, to generate the force graph in a 3D graph.

$$\begin{aligned}
 curve(\alpha_1) &= \begin{bmatrix} \alpha_1 \\ v_1(\alpha_1) \\ F_1(\alpha_1) \end{bmatrix} & curve(\alpha_2) &= \begin{bmatrix} \alpha_2 \\ v_2(\alpha_2) \\ F_2(\alpha_2) \end{bmatrix} \\
 \alpha_{10} &:= 0.0001 & \alpha_{20} &:= \frac{\pi}{4} \\
 \alpha_{11} &:= \frac{\pi}{4} & \alpha_{21} &:= \frac{\pi}{2} \\
 S1 &:= CreateSpace(curve, \alpha_{10}, \alpha_{11}, 50) & S2 &:= CreateSpace(curve, \alpha_{20}, \alpha_{21}, 50) \\
 curve(\alpha_3) &= \begin{bmatrix} \alpha_3 \\ v_3(\alpha_3) \\ F_3(\alpha_3) \end{bmatrix} & curve(\alpha_4) &= \begin{bmatrix} \alpha_4 \\ v_4(\alpha_4) \\ F_4(\alpha_4) \end{bmatrix} \\
 \alpha_{30} &:= \frac{\pi}{2} & \alpha_{40} &:= \frac{3\pi}{4} \\
 \alpha_{31} &:= \frac{3\pi}{4} & \alpha_{41} &:= \pi + 0.001 \\
 S3 &:= CreateSpace(curve, \alpha_{30}, \alpha_{31}, 50) & S4 &:= CreateSpace(curve, \alpha_{40}, \alpha_{41}, 50)
 \end{aligned}$$

Figure 8 Creation of the linear space in Mathcad

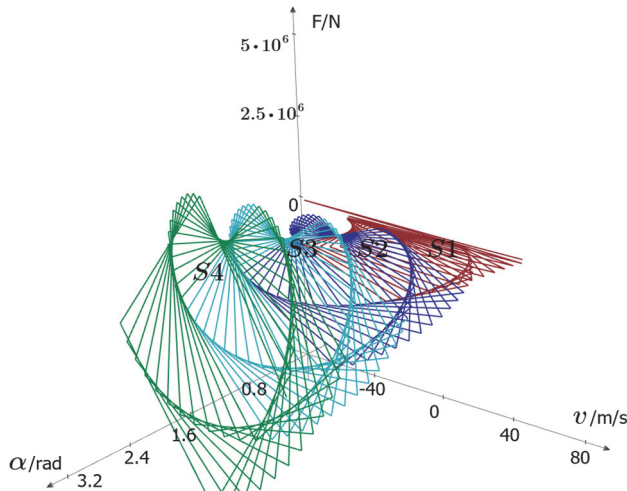


Figure 9 Dependence of force on angle of rotation and linear speed of movement of the module

Finally, the graph in Fig. 9 resulted, which has on the Ox axis the time formed by, $\alpha[\text{rad}] = \{\alpha_1, \alpha_2, \alpha_3, \alpha_4\}$ on the Oy axis it has the velocity formed by $v[\text{m/s}] = \{v_1(\alpha_1), v_2(\alpha_2), v_3(\alpha_3), v_4(\alpha_4)\}$, and on the Oz axis the inertia force of the 4 working intervals $F[\text{N}] = \{F_1(\alpha_1), F_2(\alpha_2), F_3(\alpha_3), F_4(\alpha_4)\}$.

Using the 3D plotting formulas in MathCAD it can be seen that the total inertia force is positive when the sum of the accelerations of the different centers of gravity of all chain portions and/or a mass variation given by the constructive shape of the device with weights is distributed over half the length of the chain.

3 CONCLUSIONS

The effect of inertial forces in the direction perpendicular to the direction of travel was not studied in the paper.

These forces also exist at full rotation of the frame 6 having a sinusoidal oscillation, they oscillate at full rotation from a positive maximum value to a negative

maximum value. In order to eliminate this impediment, if we use two chain drives with identical weights, but symmetrically placed, as shown in the attached figure, with respect to the axis $O-O_1$, their sum is zero, which justifies not taking them into account.

In the case of a single-chain system, the operation of the system is subject to vibrations, which are eliminated by using the system described in the previous figure (with two chains).

The four-module system is used to compensate for the lateral movement of the vehicle on which it is mounted and to maintain the resulting positive force in the direction of movement.

The entire study was done in the situation where the device on which the inertial system is mounted is moving with constant linear velocity along the direction of travel, so the acceleration of the device is zero.

In the case of a speed change, as well as in the case of departure from the start, in the calculation, this speed change must also be taken into account, namely a non-zero acceleration, positive or negative depending on acceleration or deceleration.

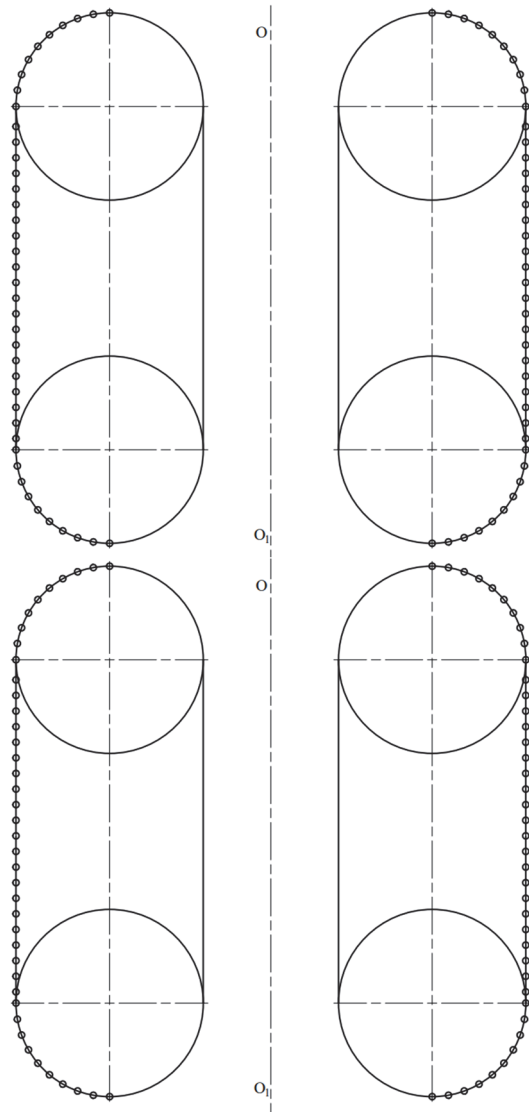


Figure 10 Two chain drives with identical weights

In this case, the formula for the total traction force also includes $F = m_d \cdot a$ the required force with a positive sign

in the case of decelerations and a negative sign in the case of accelerations. In this formula m_d represents the total mass of the device together with the inertial system and a represents the acceleration of the whole device.

The program made in Mathcad, the 3D drawing of the mechanism made in SolidWorks and the part of the drawings made in AutoCAD can be accessed on the following link:

<https://drive.google.com/drive/folders/1g2jaJZRyuiFsV7ANfa4fw0pSdKJjJQs?usp=sharing>

The practical use of this inertial device would be in the case of passenger cars, especially in winter conditions to avoid skidding, but also on locomotives with large gauge dimensions, allowing the mounting of this device on a large scale to obtain traction force proportional to the gauge.

4 REFERENCES

- [1] Leech, C. M. (2014). Contact Force and Friction. *Book Series Solid Mechanics and its Applications*, 91-113. https://doi.org/10.1007/978-94-007-7841-2_7
- [2] Gerochs, A. (2020). The Kinematic and Dynamic Study of an Inertial Propulsion System Based on Rotating Masses. *ACTA Polytechnica Hungarica*, 17(6), 225-237. <https://doi.org/10.12700/APH.17.6.2020.6.13>
- [3] Ciulin, D. (2008). System to Produce Mechanical Inertial Force and/or Torque. *Conference Meeting International Joint Conference on Computer, Information, Systems Sciences and Engineering*, 51-56. https://doi.org/10.1007/978-90-481-3656-8_11
- [4] Kovecses, J. (2010). Unit homogenization for estimation of inertial parameters of multibody mechanical systems. *Mechanism and Machine Theory*, 45(3), 438-453. <https://doi.org/10.1016/j.mechmachtheory.2009.10.004>
- [5] Ouyang, C., Shi, S., You, Z., & Zhao, K. (2019). Extrinsic Parameter Calibration Method for a Visual/Inertial Integrated System with a Predefined Mechanical Interface. *Sensors*, 19(14). <https://doi.org/10.3390/s19143086>
- [6] Yuan, C., Lai, J., Lyu, P., Shi, P., Zhao, W., & Huang, K. A. (2018). Novel Fault-Tolerant Navigation and Positioning Method with Stereo-Camera/Micro Electro Mechanical Systems Inertial Measurement Unit (MEMS-IMU) in Hostile Environment. *Micromachines*, 9(12), 626. <https://doi.org/SENSORS10.3390/mi9120626>
- [7] Booden J. D. (1998). United States of America Patent No. US Patent 5782134.
- [8] Gerochs, A., Gillich, G., Nedelcu, D., & Korka, Z. (2020). A Multibody Inertial Propulsion Drive with Symmetrically Placed Balls Rotating on Eccentric Trajectories. *Symmetry-Basel*, 12(9). <https://doi.org/10.3390/sym12091422>
- [9] Korka, Z., Cojocaru, V., & Miclosina, C. (2019). Modal - Based Design Optimization of a Gearbox Housing. *Romanian Journal of Acoustics and Vibration*, 16(1), 58-65.
- [10] Gillich, G., Furdui, H., Wahab, M., & Korka, Z. (2017). A robust damage detection method based on multi-modal analysis in variable temperature conditions. *Conference on Structural Engineering Dynamics (ICEDyn)*, 115, 361-379. <https://doi.org/10.1016/j.ymssp.2018.05.037>
- [11] Mot, L. G. (2000). *Superior mathematics for engineers and economists* (2nd ed.). Arad: Life in Arad.

Contact information:

Attila GERÖCS, University Lecturer
University Aurel Vlaicu of Arad, Faculty of Engineering,
B-dul Revoluției Nr. 77, România. P. O. BOX 2/158 AR
E-mail: atti.gerocs@gmail.com

Elena MUNCUT (WISZNOVSZKY), University Lecturer
(Corresponding author)
University Aurel Vlaicu of Arad, Faculty of Engineering,
B-dul Revoluției Nr. 77, România. P. O. BOX 2/158 AR
E-mail: muncutstela@yahoo.com

Andrei KOMJATY, University Lecturer
University Aurel Vlaicu of Arad, Faculty of Engineering,
B-dul Revoluției Nr. 77, România. P. O. BOX 2/158 AR
E-mail: komjatya@gmail.com

Ramona LILE, University Professor
University Aurel Vlaicu of Arad, Faculty of Economics,
B-dul Revoluției Nr. 77, România. P. O. BOX 2/158 AR
E-mail: ramona.lile@uav.ro

István BíRÓ, University Professor
University of Szeged, Faculty of Engineering,
Mars tér 7, H-6724 Szeged, Hungary
E-mail: biro-i@mk.u-szeged.hu